Copy
RM L56J18

NACA RM L56J18

NACA

RESEARCH MEMORANDUM

TRANSONIC AND SUPERSONIC CHARACTERISTICS OF A HORN-BALANCED CONTROL WITH UNBALANCING TAB ON A 55° SWEPTBACK WING

By Lawrence D. Guy

Langley Aeronautical Laboratory
Langley Field, Va.

NATIONAL ADVISORY COMMITTEE
FOR AERONAUTICS

WASHINGTON

January 15, 1957

NACA RM L56J18

NATIONAL ADVISORY COMMITTEE FOR AERONAUTICS

RESEARCH MEMORANDUM

TRANSONIC AND SUPERSONIC CHARACTERISTICS OF A HORN-BALANCED CONTROL WITH UNBALANCING TAB ON A 55° SWEPTBACK WING

By Lawrence D. Guy

SUMMARY

An exploratory investigation of a semispan-wing—fuselage model having a 55° sweptback triangular wing of aspect ratio 3.5 with a horn-balanced, flap-type control equipped with a partially inset unbalancing tab was conducted in the Langley 9- by 12-inch blowdown tunnel. Control hinge-moment and effectiveness characteristics were obtained over an angle-of-attack range of ±10° at flap deflections up to 10° and tab deflections up to 6°. Data were obtained at Mach numbers from 0.71 to 1.96 for Reynolds numbers between 1.9×10^6 and 2.5×10^6. No detailed analysis of the data is presented.

INTRODUCTION

At the very high flight speeds of present-day aircraft and missiles the forces and moments required to actuate control surfaces have become very large in magnitude. Various means have been used to balance, aerodynamically, control-hinge moments at either subsonic or supersonic speeds. However, the rearward shift in center of pressure at transonic speeds has made the problem of achieving balanced hinge moments throughout the speed range difficult. Such was the case for the horn-balanced, flap-type control of reference 1, which was mounted on a 55° swept pointed wing. This control, although nearly balanced at supersonic speeds, was greatly overbalanced at subsonic speeds. It appeared that addition of an unbalancing tab offered a means of reducing the large overbalanced hinge moments at subsonic speeds without greatly changing the control hinge-moment characteristics at supersonic speeds, since tabs, in general, have shown sizeable losses in effectiveness at transonic speeds (refs. 2 and 3, for example). Such an arrangement would have an additional advantage in that the tab lift would add to the control lift instead of subtracting from it as in the case of a conventional tab. In order to obtain further information on such a control-tab

arrangement as well as to determine the transonic hinge-moment and effectiveness characteristics of the horn-balanced control, which were not obtained in reference 1, an exploratory investigation has been carried out in the Langley 9- by 12-inch blowdown tunnel at transonic and supersonic speeds. The 55° swept-pointed-wing model was the same as that of reference 1, and for the present investigation the horn-balanced control was equipped with a partially inset tab.

Hinge-moment and effectiveness characteristics of the control with tab were obtained over an angle-of-attack range of ±10° for flap deflections up to 10° and tab deflections up to 6°. The tests were made at Mach numbers from 0.71 to 1.96 for a range of Reynolds numbers between 1.9×10^6 and 2.5×10^6. No detailed analysis of the data is presented.

SYMBOLS

C_L	lift coefficients, $\frac{\text{Lift}}{qS}$
$C_{l_{gross}}$	gross rolling-moment coefficient (reference axis shown in fig. 1), $\frac{\text{Semispan-wing—fuselage model rolling moment}}{2qSb}$
C_m	pitching-moment coefficient (pitching-moment reference axis located at $0.25\bar{c}$ of wing), $\frac{\text{Pitching moment}}{qS\bar{c}}$
C_h	control hinge-moment coefficient, $\frac{\text{Hinge moment}}{2qb_f\bar{c}_f^2}$
$C_l, \Delta C_L, \Delta C_m$	increment in gross rolling-moment coefficient, lift coefficient, and pitching-moment coefficient, respectively, due to deflection of control surface
q	free-stream dynamic pressure
S	semispan-wing area (including area blanketed by test body)
c	local chord of wing
$\bar{c}$	mean aerodymanic chord of wing
$\bar{c}_f$	mean aerodynamic chord of portion of control behind hinge line (not including tab)

[redacted]

c_f	flap chord
b	wing span (twice distance from rolling-moment reference axis to wing tip)
b_f	flap span, $0.60b/2$
M	Mach number
ΔM	maximum deviation from average test-section Mach number
R	Reynolds number
α	wing angle of attack measured with respect to free stream
δ_f	flap deflection relative to wing chord plane (measured in plane normal to flap hinge axis), deg
δ_t	tab deflection relative to flap chord plane (measured in plane normal to tab hinge axis), deg

Subscripts:

α	partial derivative of coefficient with respect to α
δ	partial derivative of coefficient with respect to δ

DESCRIPTION OF MODELS

The principal dimensions of the semispan-wing—body combination, which was the same as that of reference 1, are shown in figure 1, and a photograph of the model without tab is presented as figure 2. The semispan wing was of triangular plan form having a 55° leading-edge sweepback and an aspect ratio of 3.5. A horn-balanced, flap-type control was hinged at the 70-percent chord line and spanned the outboard 60 percent of the wing semispan. The horn-balance surface comprised the full-wing chord of the outboard 30 percent of the semispan. A test body, consisting of a half-body of revolution together with a 0.25-inch shim was fastened to the wing for all tests.

The wing and control surface were both machined of heat-treated steel. The wing ahead of the control surface had NACA 65A005 airfoil sections parallel to the free-stream direction. Inboard of the control surface the wing thickness was increased to the rear of the 20-percent-chord station to permit installation of an internal strain gage. Ordinates are given in reference 1.

The control surface had NACA 65A005 airfoil sections forward of the hinge line but was slab sided behind the hinge line with a trailing-edge thickness of one-half the hinge-line thickness. A portion of the flap comprising the rearward 25-percent flap chord and inner 26-percent flap span was cut away to permit attachment of a tab. The tab was machined of mild steel with a tongue which was inserted in a groove in the flap trailing edge and sweated in place. (See fig. 1.) The tab chord was 35 percent of the flap chord and extended $0.10c_f$ rearward of the wing trailing edge.

A small fence was mounted on the wing at the outboard wing-control parting line (see figs. 1 and 2).

TEST TECHNIQUE

The semispan model was cantilevered from a five-component strain-gage balance set flush with the tunnel floor. The aerodynamic forces and moments on the semispan-wing—body combination were measured with respect to the body axes and then were transferred to the wind axes. The 0.25-inch shim was used to minimize the effects of the tunnel-wall boundary layer on the flow over the surface of the body of revolution (refs. 4 and 5). A clearance gap of 0.010 inch to 0.020 inch was maintained between the fuselage shim and the tunnel floor.

The hinge moments of the control surface were measured by means of an electrical strain-gage beam buried in the main wing panel adjacent to the inboard end of the control surface. The control was hinged to the main wing panel by a 0.030-inch-diameter steel pin just inboard of the control balance area and by a 0.060-inch-diameter steel pin at its inboard end. The control was restrained by a positioning pin soldered to the control surface and fitted into a hole in the strain-gage beam. Deflection of the tab was accomplished by bending the tab tongue about its juncture with the flap. The discontinuity at the tab-flap juncture was filled with putty after bending and faired with a small radius for all tests.

TUNNEL AND TEST CONDITIONS

The tests were conducted in the Langley 9- by 12-inch blowdown tunnel which operated from the compressed air of the Langley 19-foot pressure tunnel. The absolute stagnation pressure of the air entering the test section ranged from 2 to $2\frac{1}{3}$ atmospheres. The compressed air was conditioned to insure condensation-free flow in the test section

by being passed through a silica-gel drier and then through banks of finned electrical heaters. Criteria for condensation-free flow were obtained from reference 6. Turbulence damping screens were located in the settling chamber. Three interchangeable nozzle blocks provided test-section Mach numbers of 0.70 to 1.25, 1.41, and 1.96.

Transonic Nozzle

A description of the transonic nozzle, which has a 7- by 10-inch test section, together with a discussion of the flow characteristics obtained from calibration tests is presented in reference 7. Satisfactory test-section flow characteristics are indicated from the minimum Mach number ($M \approx 0.7$) to about $M = 1.25$. The maximum deviations from the average Mach number in the region occupied by the model are shown in figure 3(a). Limited tests indicated that the stream angle probably did not exceed $\pm 0.1^{\circ}$ at any Mach number. During tests the test-section flow was maintained within ± 0.005 of the desired Mach number by an electronically controlled device. The variation with Mach number of the average Reynolds number of the tests is given in figure 3(b).

Supersonic Nozzles

Test-section flow characteristics of the three supersonic fixed Mach number nozzles, which had 9- by 12-inch test sections, were determined from extensive calibration tests and are reported in reference 8. Deviation of flow conditions in the test section with tunnel clear are presented in the following table:

Average Mach number	1.41	1.96
Maximum deviation in Mach number	±0.02	±0.02
Maximum deviation in stream angle, deg	±0.25	±0.20
Average Reynolds number (approx.)	2.3×10^6	2.0×10^6

Accuracy and Limitation of Data

An estimate of the probable errors introduced in the present data by instrument-reading errors, measuring-equipment errors, and calibration errors are presented in the following table:

C_L	±0.006
C_l	±0.0005
C_m	±0.001
C_h	±0.005

α, deg	± 0.1
δ_f, deg	± 0.2
δ_t, deg	± 0.1

The flap deflection was measured at a point on the control trailing edge adjacent to the main wing panel while the tab deflection, relative to the flap, was measured by an optical method. Determination of the mean angular deflection of the control due to load was not attempted. (See ref. 1.)

It is believed that the increased thickness of the wing inboard of the control had negligible effect on control characteristics at supersonic speeds. The effects at transonic speeds are unknown.

Data obtained in the transonic nozzle are subject to various jet-boundary interference effects throughout the usable speed range. Blockage interference is believed to be minimized by the nozzle slot configuration. However, reflection-plane and lift interferences at high subsonic speeds and wave reflection interference at low supersonic speeds still exist. This imposes certain limitations on the data, particularly the loadings due to angle of attack which are discussed in references 7 and 9. In general, however, the control characteristics due to angle of attack are believed reliable except between Mach numbers 0.94 and 1.04, whereas the control characteristics due to deflection are believed reliable at all Mach numbers presented insofar as boundary induced disturbances are concerned. For detailed discussion see references 7 and 9. In the fixed Mach number nozzles (M = 1.41 and higher), the models were clear of reflected disturbances.

RESULTS

The aerodynamic characteristics including hinge-moment coefficient of the horn-balanced, flap-tab combination are presented in figures 4 and 5 for Mach numbers of 0.71 and 1.41, respectively. These data are representative of the quality of the basic data obtained in this investigation; however, the tab deflections given are only nominal values as the deflections were not constant at the values shown. For subsequent figures it was necessary to cross plot the data against tab deflection for constant values of flap deflection obtained from plots similar to these. Figure 6 presents plots against control deflection of the rolling-moment coefficients and the increments in lift and pitching-moment coefficients due to deflection of the control for $\delta_t = 0$ and several angles of attack at Mach numbers from 0.71 to 1.96. The variation of hinge-moment coefficient with flap delection for all values of tab deflection and several angles of attack are presented in figure 7 for all Mach numbers. The data shown at negative values of flap and tab deflection were

obtained at negative angles of attack; the signs of the angles of attack and control deflection and hinge-moment coefficients have been arbitrarily reversed for convenience of presentation. At zero angle of attack, the data shown for both positive and negative control deflections were obtained from the same data points. This was permissible by reason of model symmetry. Figure 8 presents the variation of hinge-moment coefficient with angle of attack for the control undeflected at various Mach numbers. All tests were made with a small fence at the outboard wing-control parting line. This fence was shown in reference 1 to reduce the nonlinearities of hinge-moment-coefficient and rolling-moment-coefficient variations with flap deflection at supersonic speeds.

Due to the exploratory nature of the investigation, the range of flap and tab deflections for which data were obtained was restricted to only those sufficient to define trends. In figures 4 to 8 only the hinge-moment coefficients have been presented in complete form. Values of rolling-moment coefficient and increments in lift and pitching-moment coefficients due to deflection have been presented only for $\delta_t = 0$ for two reasons. At subsonic and transonic speeds the control characteristics, including hinge-moment coefficient, are believed to be of qualitative rather than quantitative value principally because of the unknown effects of the thickened inboard wing sections. Furthermore, the effectiveness of the tab in lift and roll was clearly defined only at subsonic Mach numbers. At transonic and supersonic speeds the accuracy of the measurements and the scatter or nonlinearities in the data were such that the effectiveness parameters $C_{l_{\delta_t}}$, $\Delta C_{L_{\delta_t}}$, and $\Delta C_{m_{\delta_t}}$ could not be accurately established for the small values of tab deflection of the present tests.

No corrections are available to allow for reflection-plane interference at subsonic and low supersonic Mach numbers. Some error in the absolute values of C_l, ΔC_L, and ΔC_h indicated for differentially deflected ailerons consequently is introduced. The error in differences of comparative values, however, is believed small.

Although detailed analysis of the data has not been made, some of the more significant aspects of the results are pointed out.

The previous investigation of the horn-balanced flap (without tab), reported in reference 1, was carried out only at subsonic and at supersonic speeds. The hinge-moment and effectiveness characteristics obtained at transonic speeds in the present investigation therefore supplement the data obtained for the blunt-trailing-edge control of reference 1 except as modified by the difference in control geometry due to the tab.

Figure 9 presents the variation with Mach number of hinge-moment and roll-effectiveness-slope parameters for the flap, as well as tab, for zero angles of attack and deflection.

The hinge-moment-coefficient variation with tab deflection was essentially linear up to 6° (the maximum of the tests) for all Mach numbers as indicated in figure 7 by the equal spacing of the curves at a given flap deflection. The slope of the hinge-moment-coefficient variation with tab deflection, however, varied considerably with flap deflection at transonic speeds (fig. 9). The variation with Mach number of the parameter $C_{h_{\delta_t}}$ was relatively small in that the loss in hinge-moment balancing effectiveness often associated with tabs at transonic speeds (refs. 2 and 3) did not occur, possibly because of the blunt trailing edge of the tab.

As mentioned previously, the effectiveness parameters $C_{l_{\delta_t}}$, $\Delta C_{L_{\delta_t}}$, and $\Delta C_{m_{\delta_t}}$ at transonic and supersonic speeds could not be accurately established for the small values of tab deflections of the present tests. These slopes between 0° and 6° tab deflections were, however, positive at all speeds.

Figure 10 presents values of the ratio of tab to flap deflection required for zero hinge moments due to deflection. The values of δ_t/δ_f were determined from figure 9 by means of the equation

$$\frac{dC_h}{d\delta_f} = \frac{\partial C_h}{\partial \delta_f} + \frac{\partial C_h}{\partial \delta_t}\frac{\delta_t}{\delta_f} = 0$$

Figure 10 shows that use of the tab as an unbalancing tab was limited to Mach numbers below $M \approx 0.93$ (the upper limit of positive values of δ_t/δ_f). The rapid decrease in the ratio δ_t/δ_f from positive values to nearly -1.0 at sonic speed was due principally to the large loss in effectiveness of the horn-balance surface and in part to the increased effectiveness of the tab (fig. 9). It appears that, even if the horn-balance area were increased sufficiently to overbalance the hinge moments due to flap deflection at supersonic speeds, negative values of the ratio δ_t/δ_f would still result near a Mach number of 1.0. In any event, some means of rapidly varying the ratio δ_t/δ_f at transonic speeds would be required for balanced hinge moments.

Values of δ_t/α are also presented in figure 10 and indicate the tab deflection required to balance the control hinge moments due to angle of attack for zero flap deflection. The values of the ratios δ_t/α

were obtained by means of the slope parameters of figure 9 and the equation

$$\frac{dC_h}{d\alpha} = \frac{\partial C_h}{\partial \alpha} + \frac{\partial C_h}{\partial \delta_t} \frac{\delta_t}{\alpha} = 0$$

These data show that the unbalancing tab could be used to reduce the hinge moments due to angle of attack over a wide range of Mach numbers without sacrificing control lift characteristics. It appears, however, that the variation with Mach number of the required values of δ_t/α may be too large to be practical.

Langley Aeronautical Laboratory,
National Advisory Committee for Aeronautics,
Langley Field, Va., September 28, 1956.

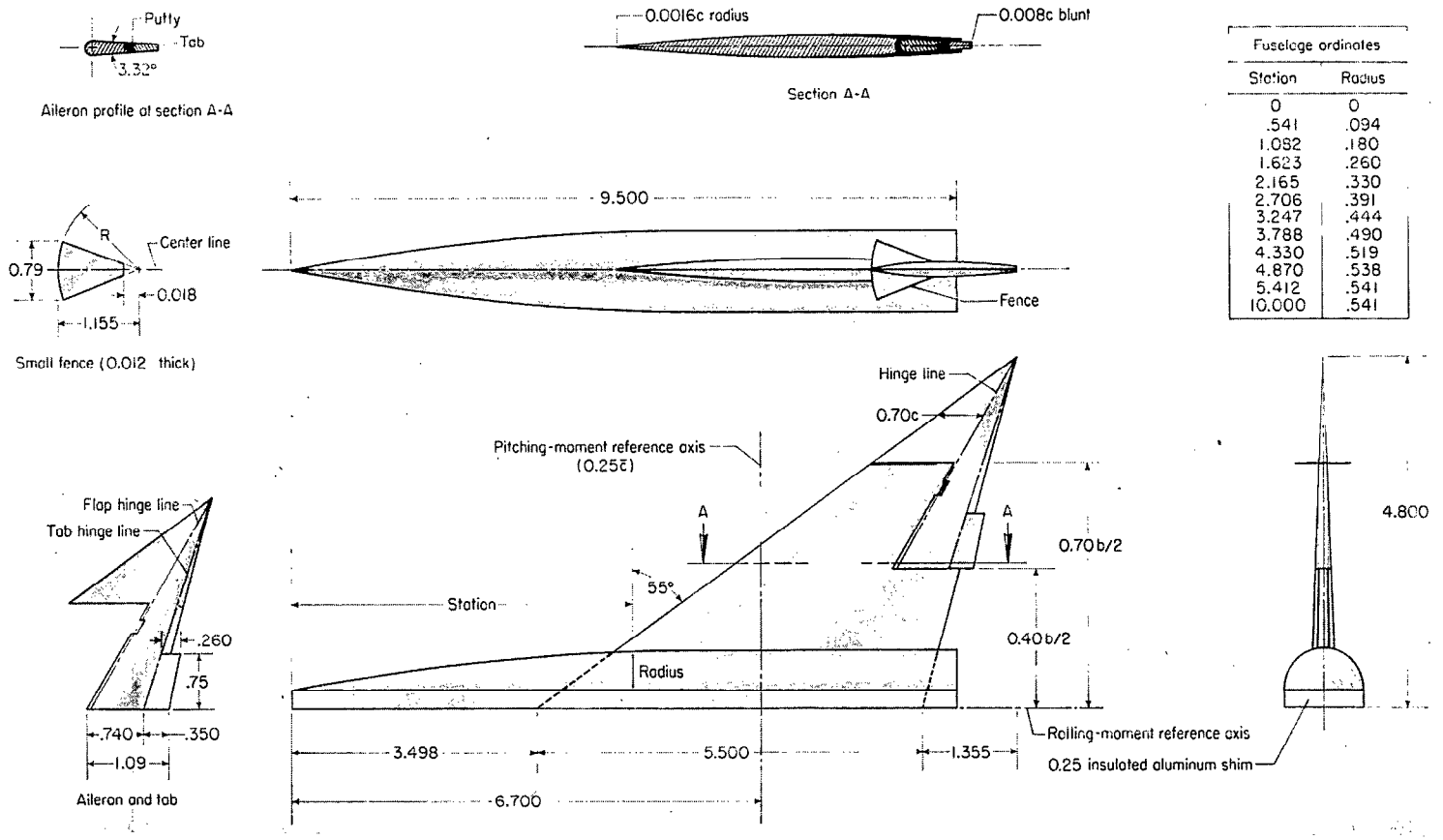

Figure 1.- Details of semispan-wing—fuselage combination. Aspect ratio, 3.5; mean aerodynamic chord, 3.667 inches; semispan-wing area, 13.20 square inches. (All dimensions are in inches unless otherwise indicated.)

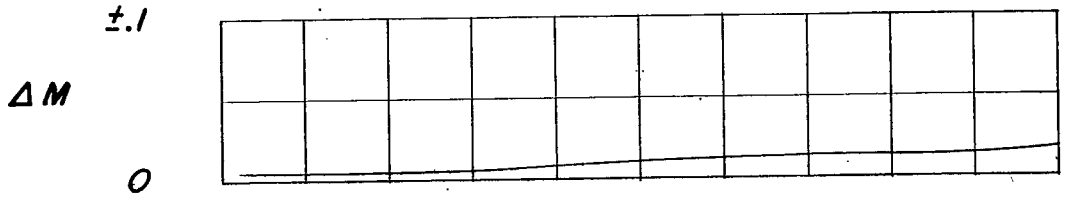

(a) Maximum deviation from average test-section Mach number.

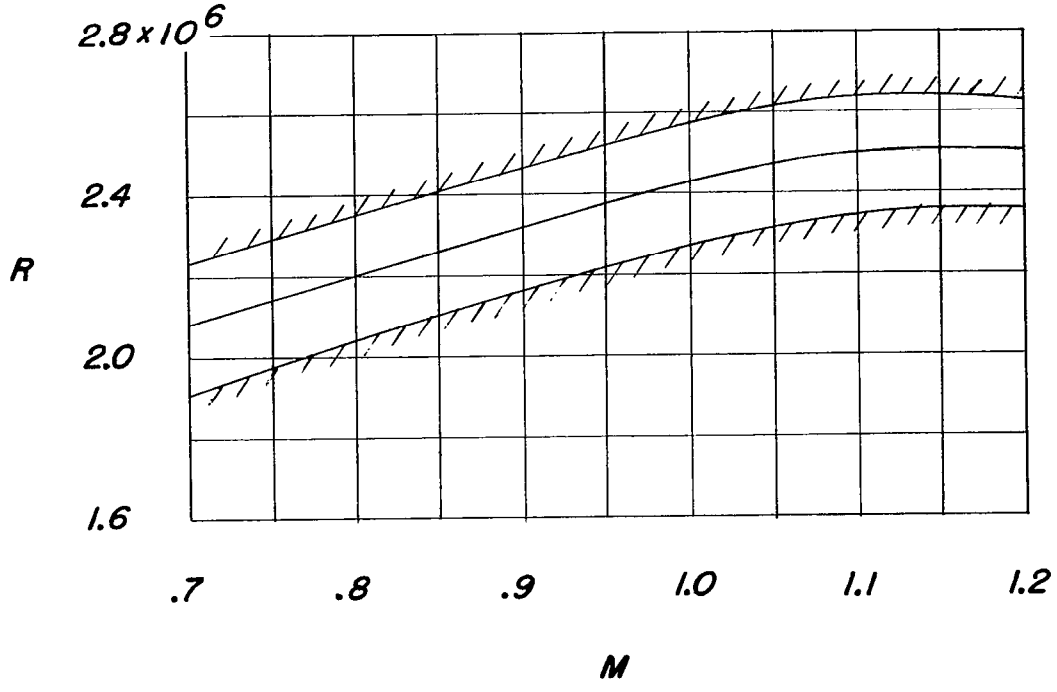

(b) Average test Reynolds number based on wing $\bar{c}$.

Figure 3.- Test-section Mach number and Reynolds number characteristics of the transonic nozzle and model.

[redacted]

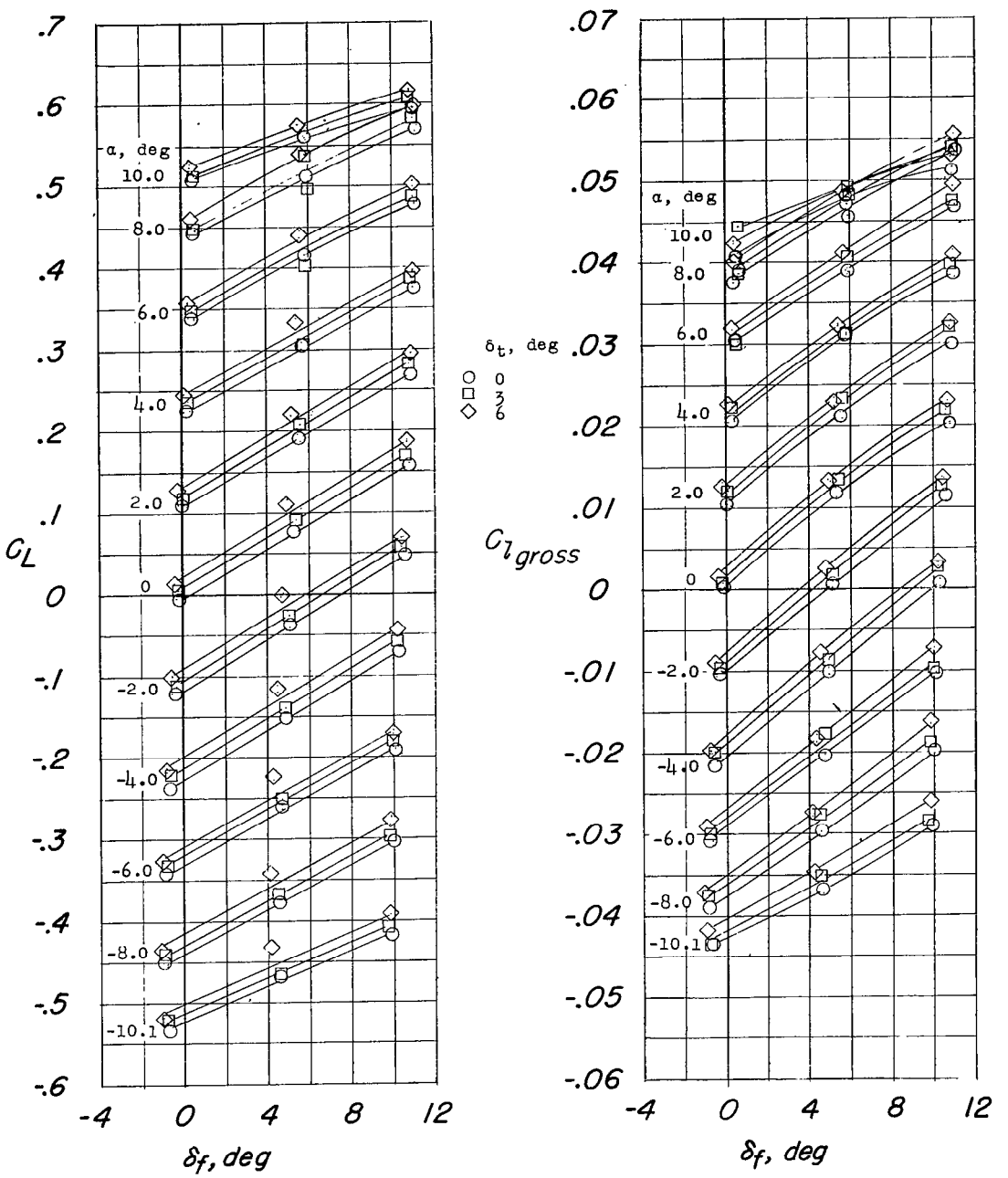

(a) C_L and C_l against δ_f.

Figure 4.- Aerodynamic characteristics, including hinge-moment coefficients, of 55° swept-pointed-wing—fuselage combination. Horn-balanced control and tab; M = 0.71.

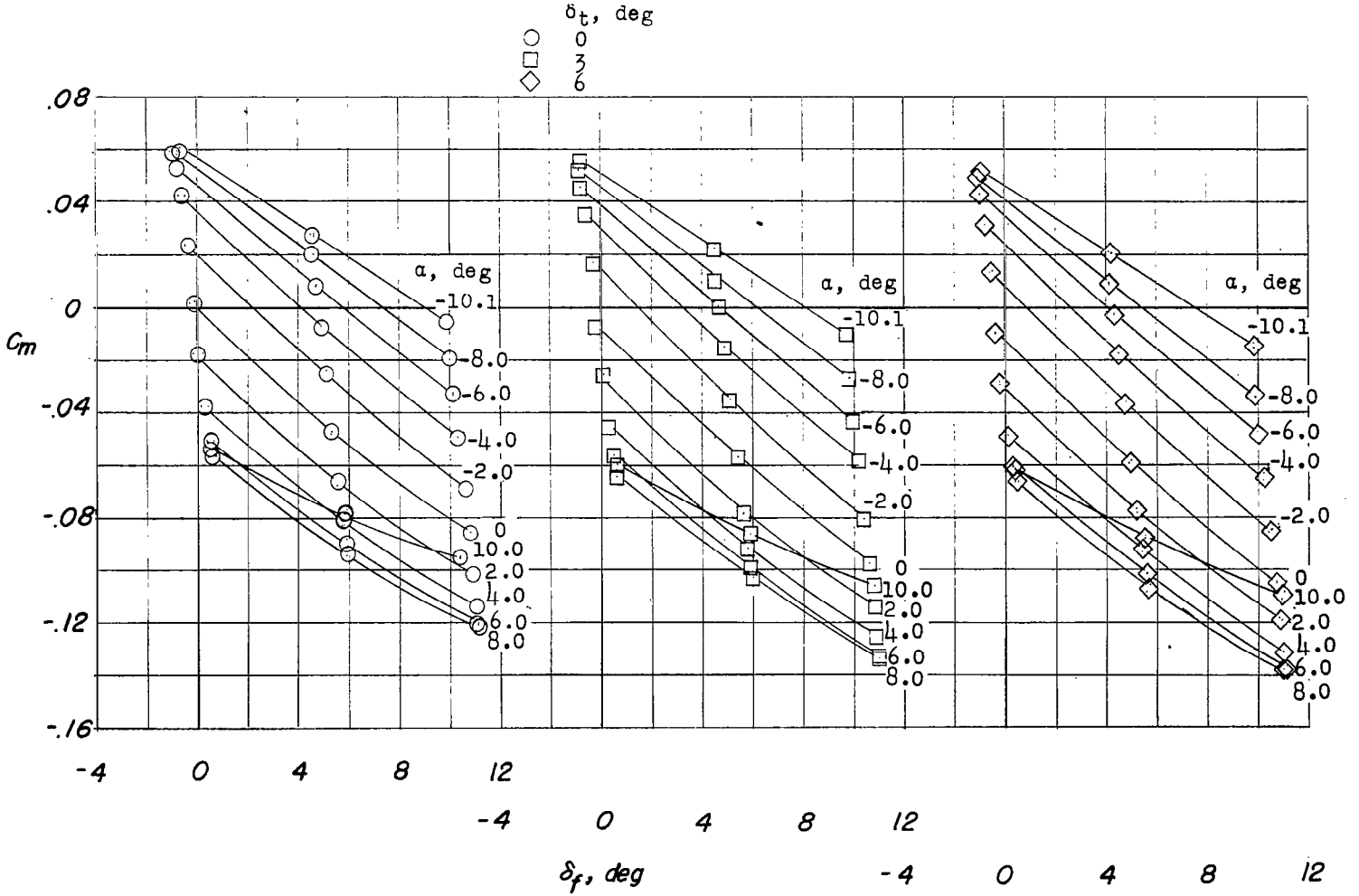

(b) C_m against δ_f.

Figure 4.- Continued.

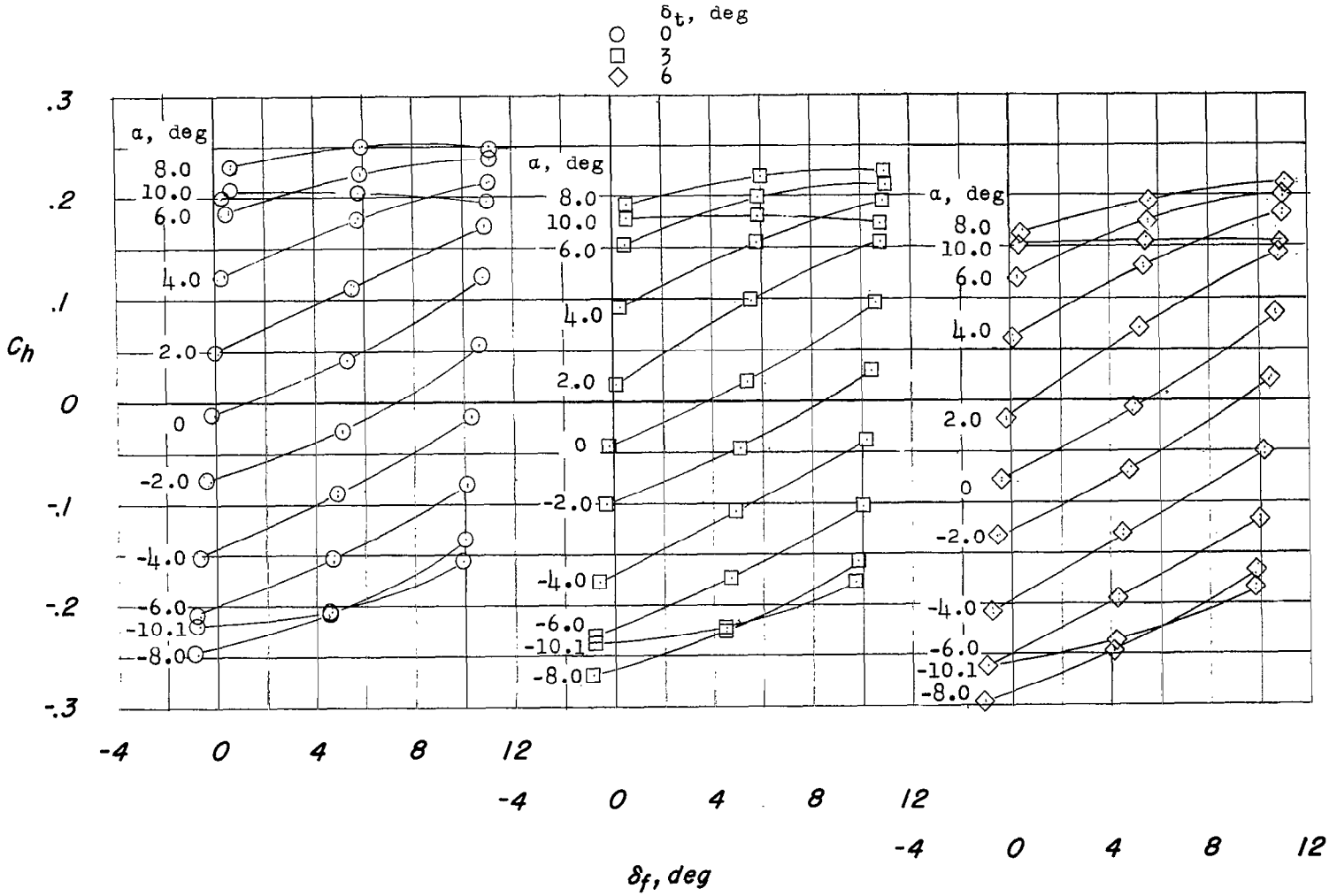

(c) C_h against δ_f.

Figure 4.- Concluded.

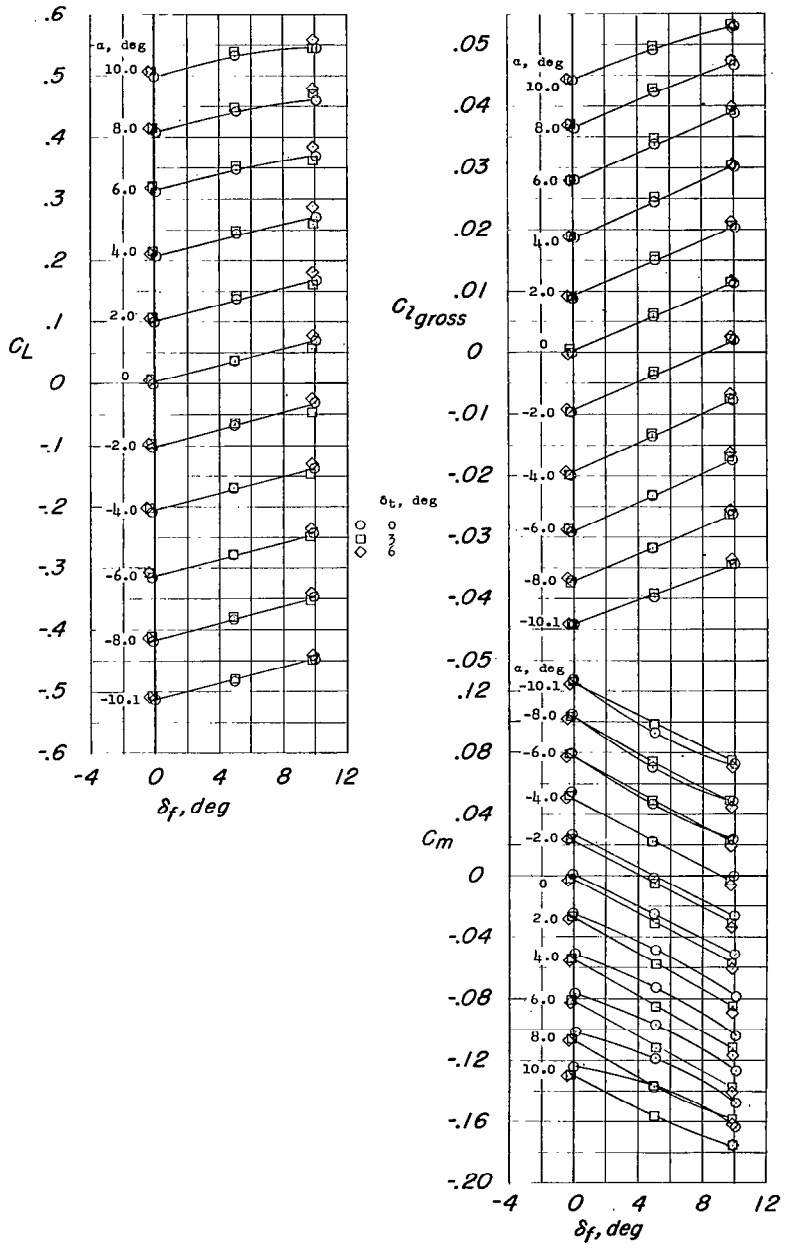

(a) C_L, C_l, and C_m against δ_f.

Figure 5.- Aerodynamic characteristics, including hinge-moment coefficients, of 55° swept-pointed-wing—fuselage combination. Horn-balanced control and tab; M = 1.41.

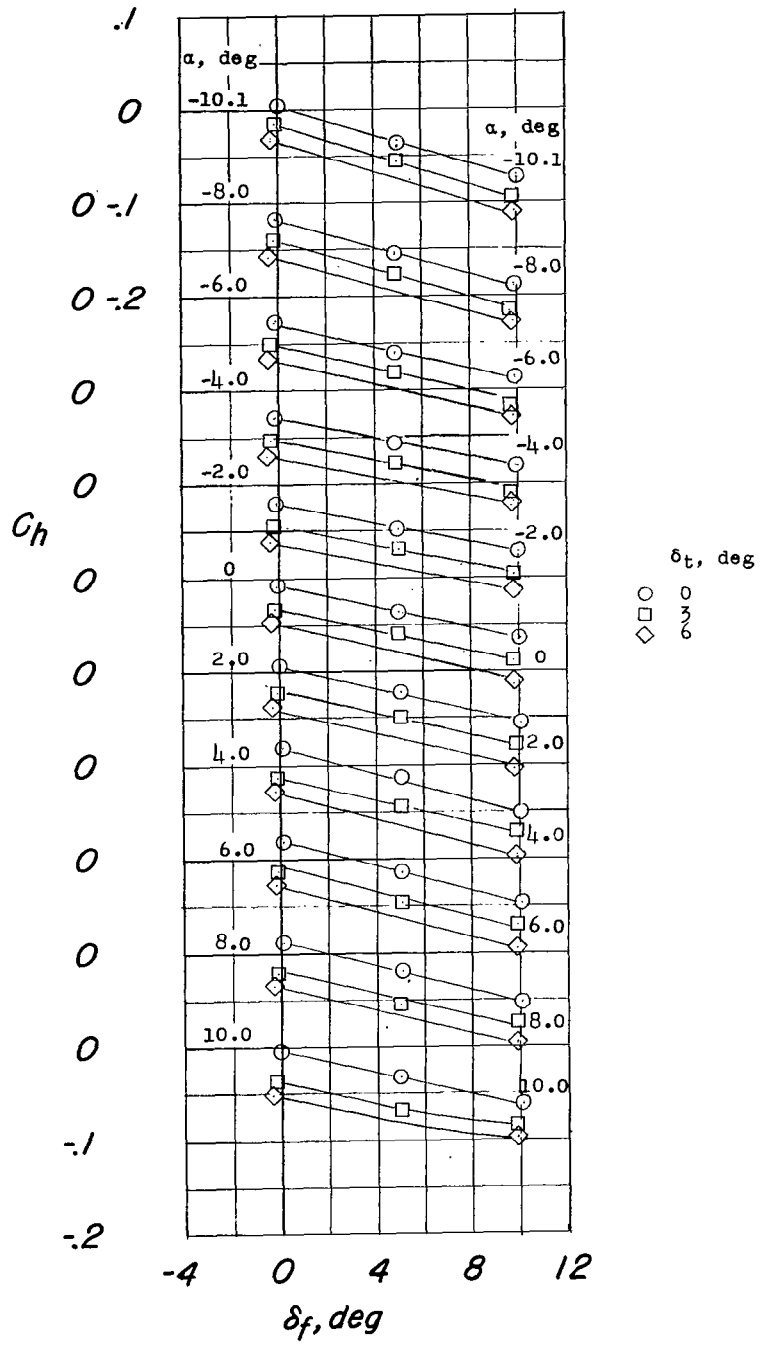

(b) C_h against δ_f.

Figure 5.- Concluded.

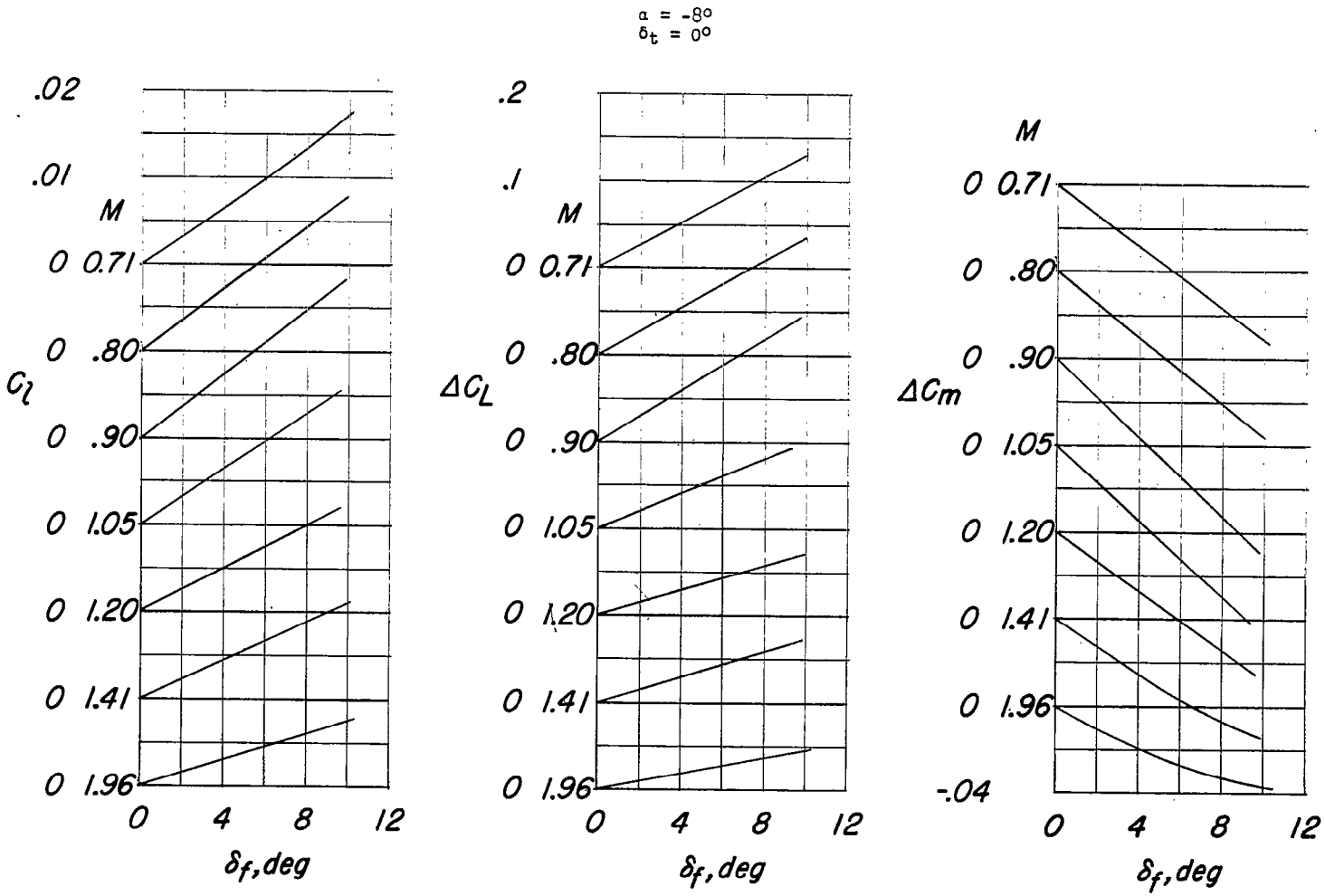

Figure 6.- Variation with flap deflection of rolling moment and increment in lift and pitching-moment coefficients due to flap deflection at various Mach numbers for three angles of attack. $\delta_t = 0^\circ$.

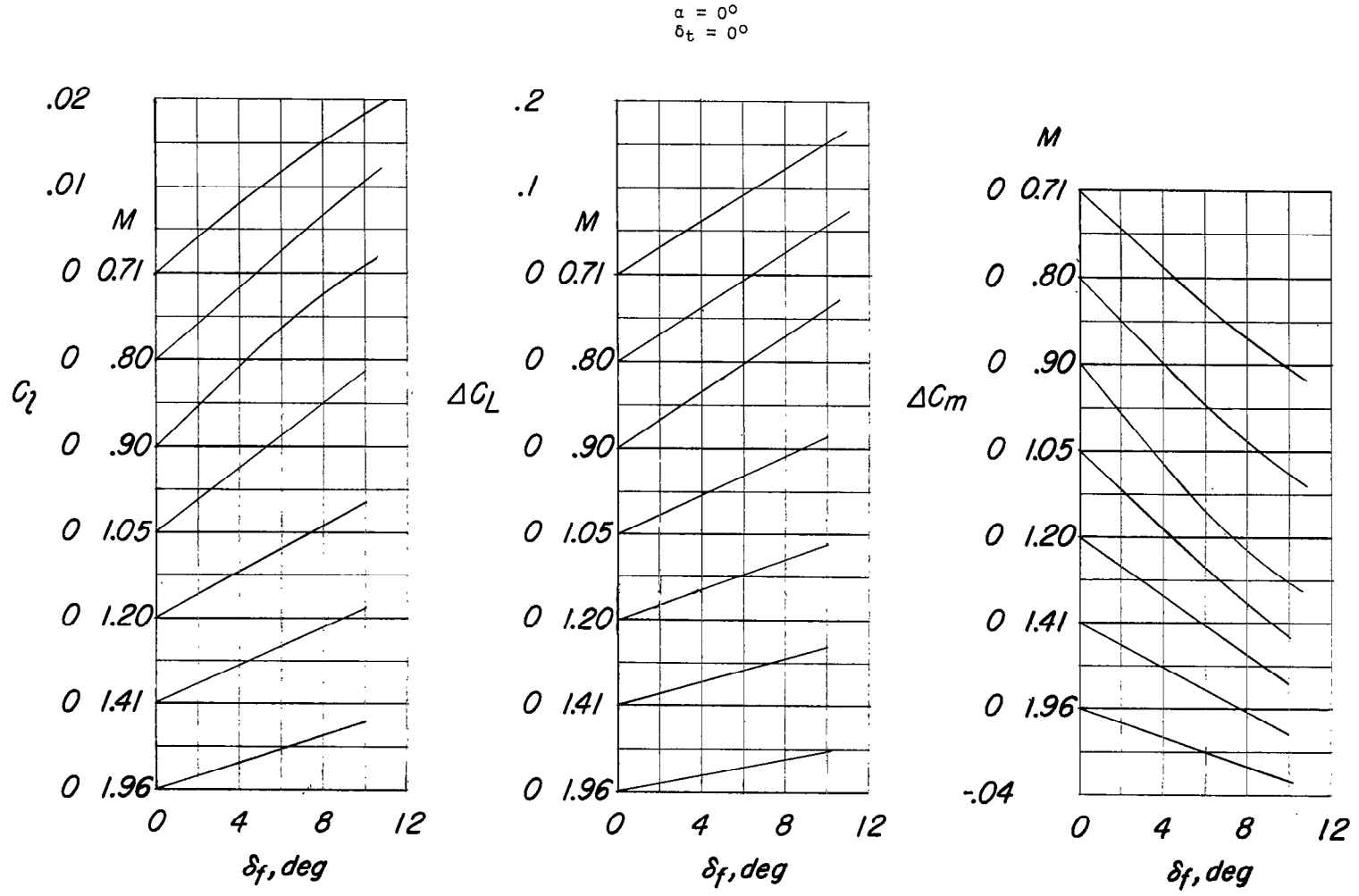

Figure 6.- Continued.

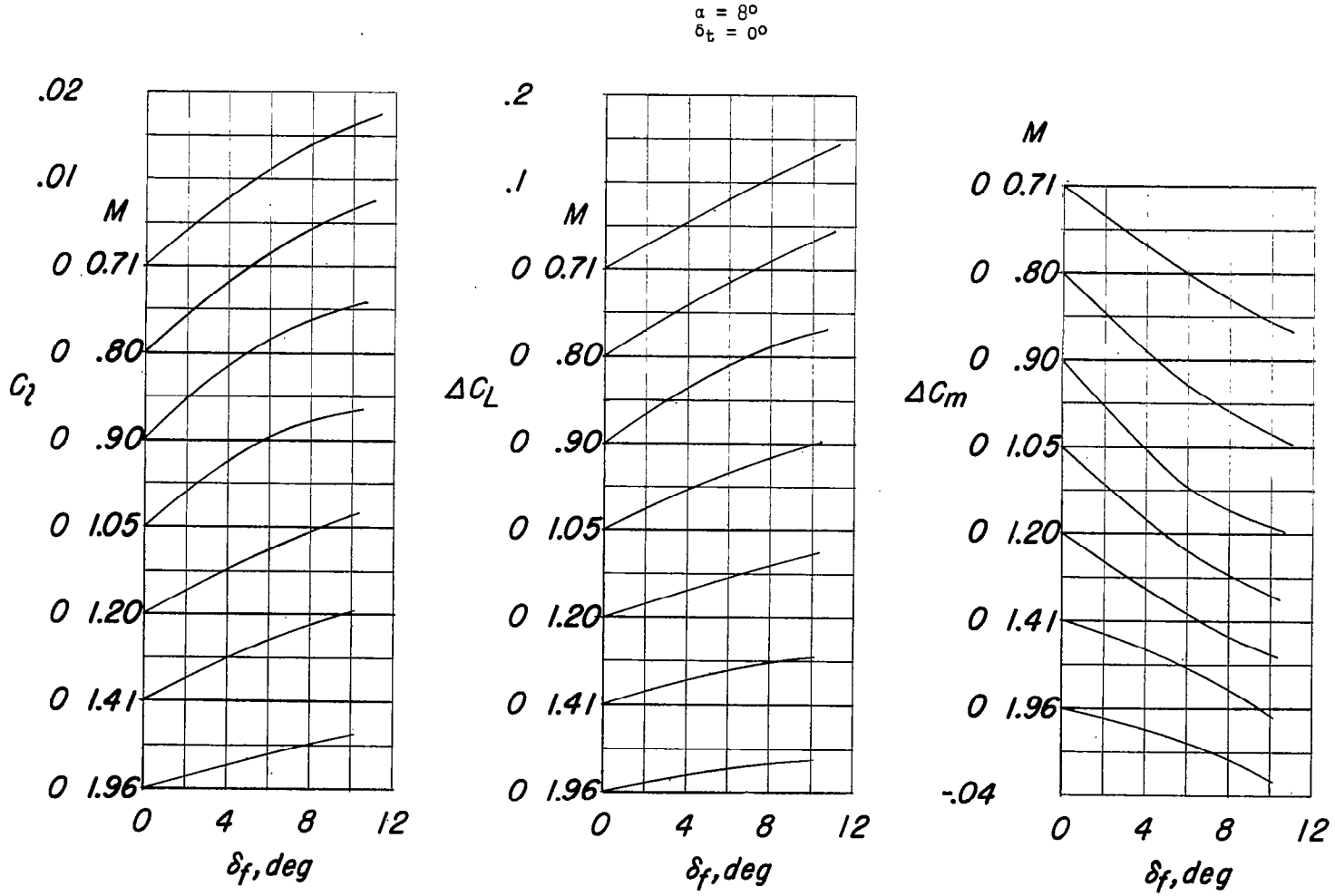

Figure 6.- Concluded.

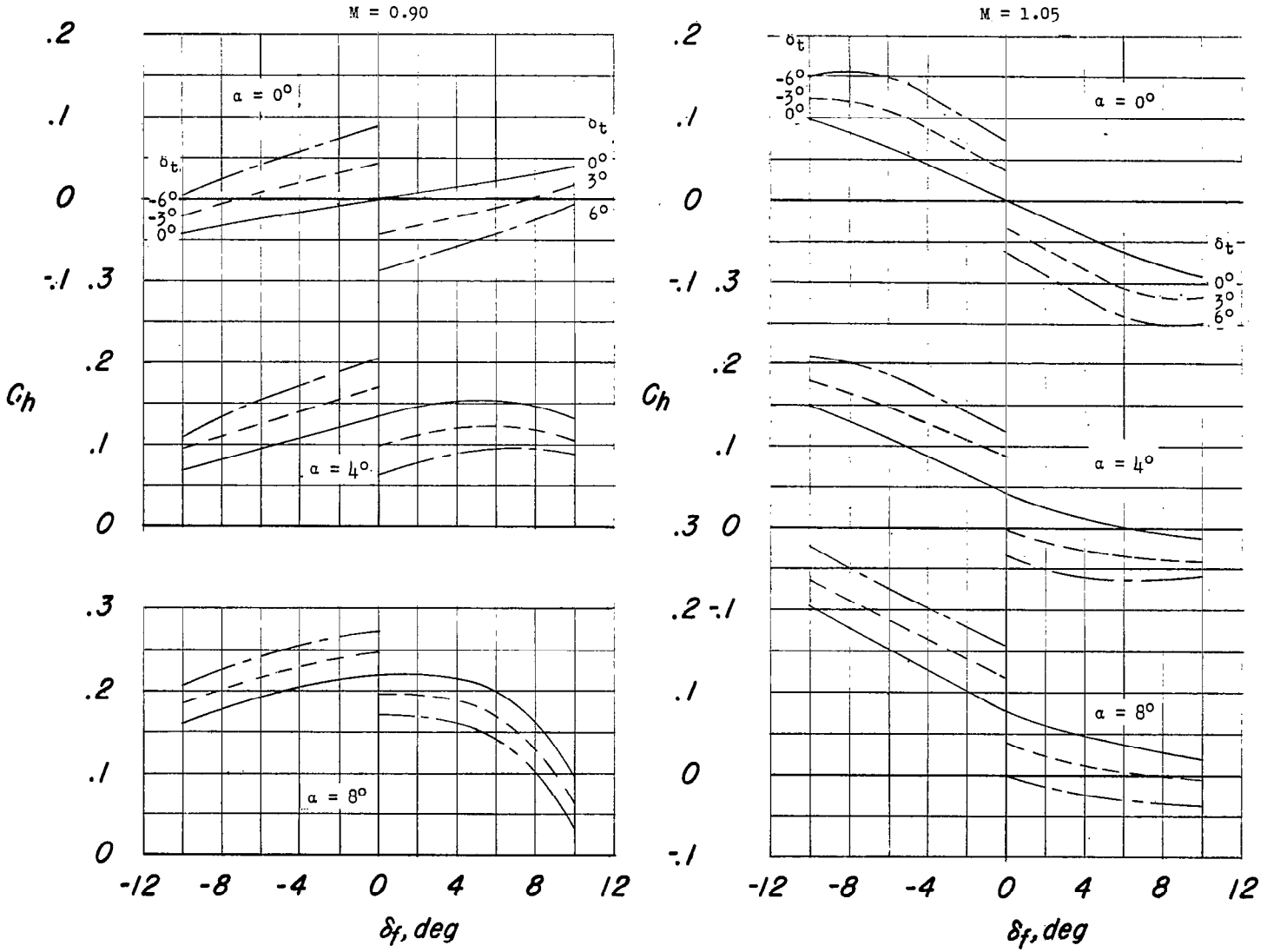

Figure 7.- Continued.

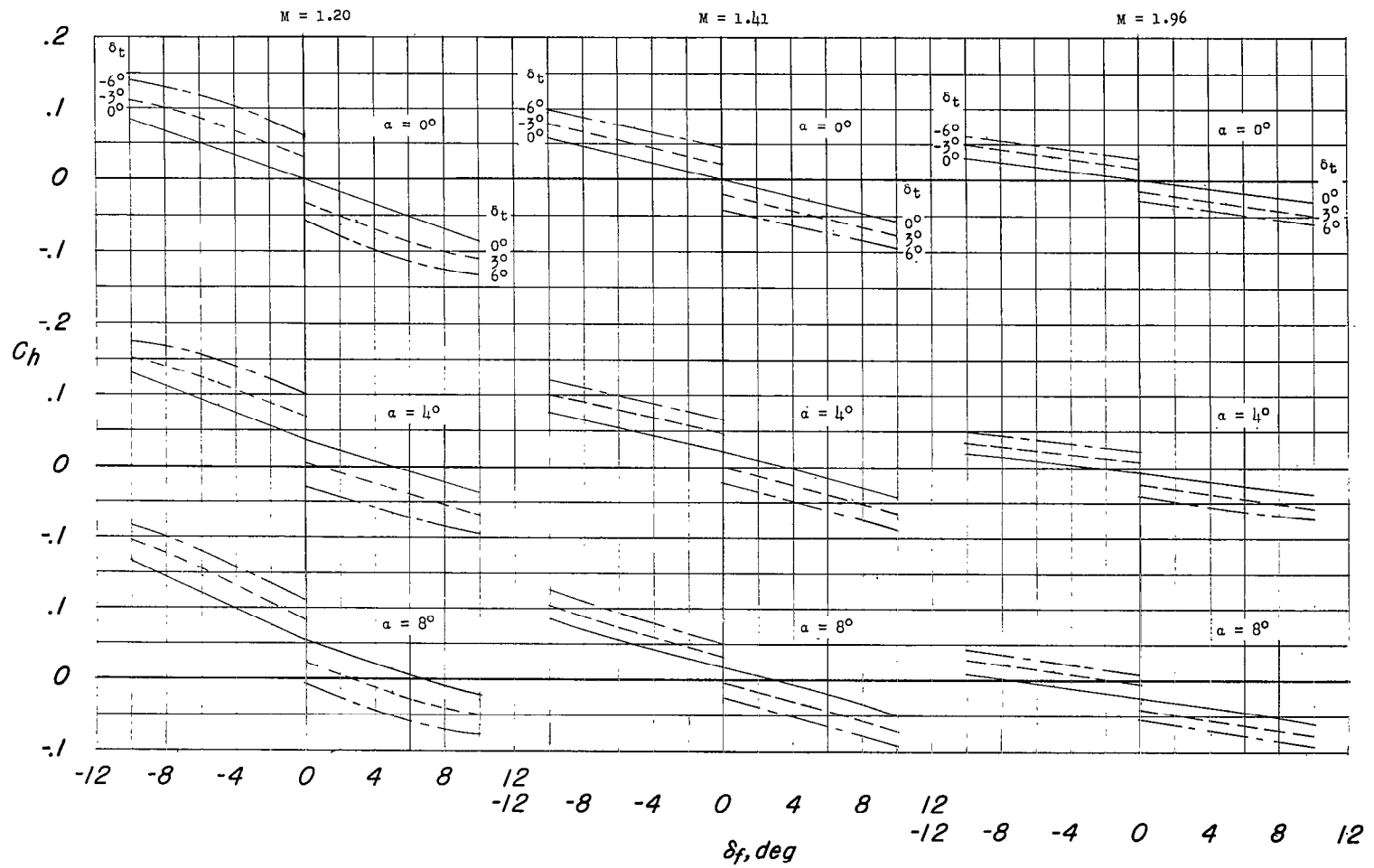

Figure 7.- Concluded.

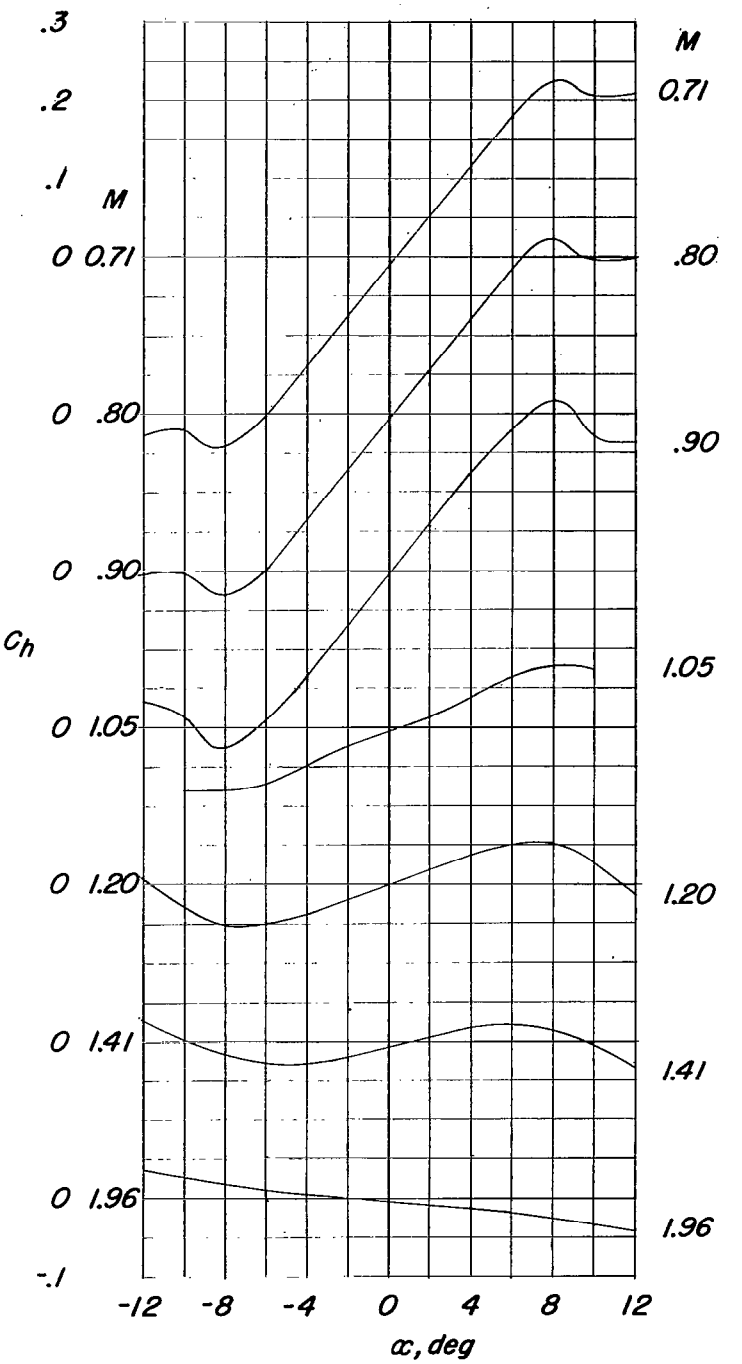

Figure 8.- Variation of hinge-moment coefficient with angle of attack. $\delta_f = 0^o$; $\delta_t = 0^o$.

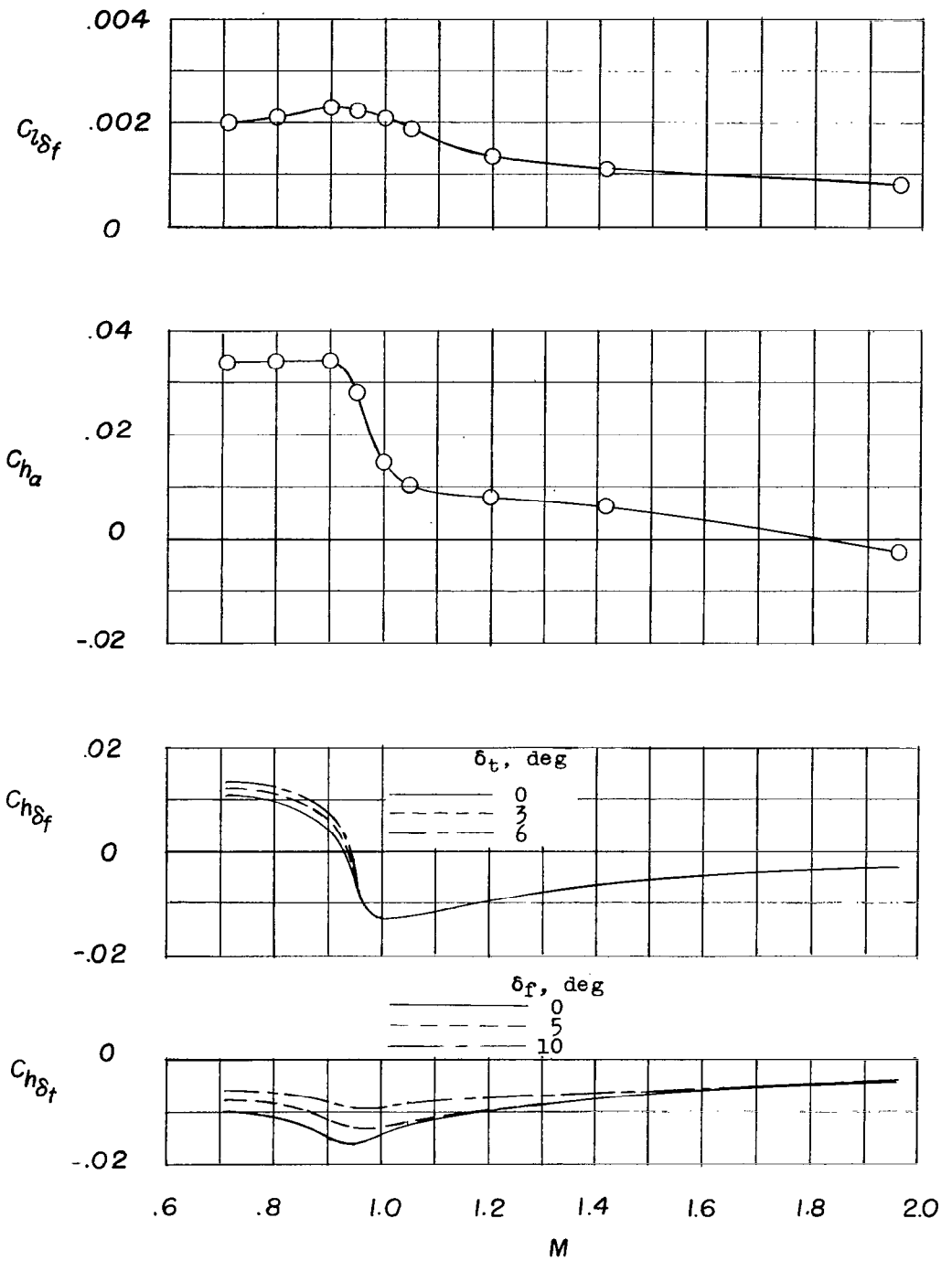

Figure 9.- Variation with Mach number of some control hinge-moment and effectiveness parameters. $\delta_f = \delta_t = \alpha = 0$ unless noted.

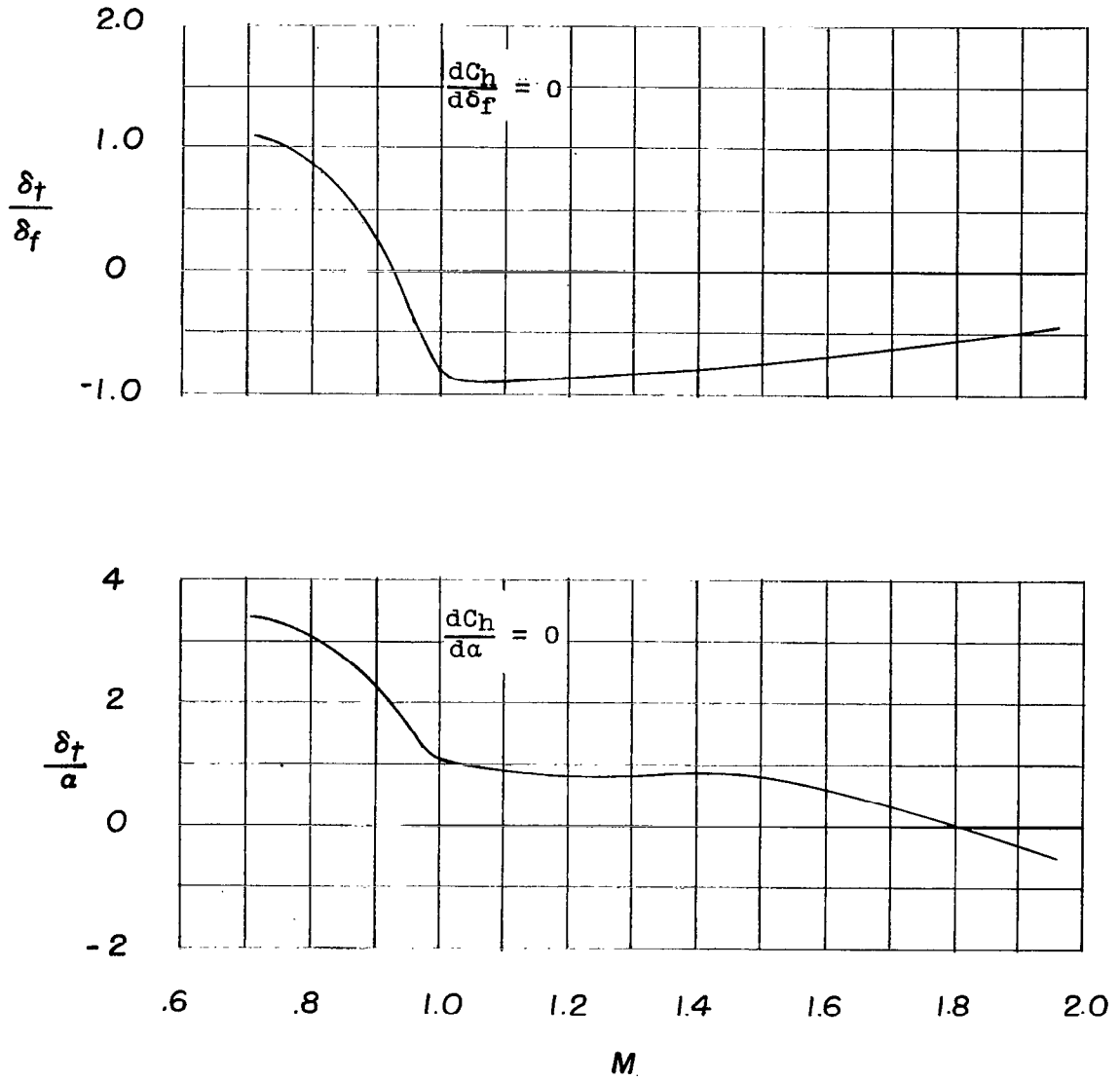

Figure 10.- Ratios of δ_t/δ_f and δ_t/α necessary to balance aerodynamically the control surface through the Mach number range.

[redacted]